Hindawi
Mobile Information Systems
Volume 2019, Article ID 7542324, 15 pages
https://doi.org/10.1155/2019/7542324

Research Article

Target Detection Coverage Algorithm Based on 3D-Voronoi Partition for Three-Dimensional Wireless Sensor Networks

Xiaochao Dang[1,2] **Chenguang Shao**[1] **and Zhanjun Hao**[1,2]

[1]*College of Computer Science and Engineering, Northwest Normal University, Lanzhou 730070, China*
[2]*Gansu Province Internet of Things Engineering Research Center, Lanzhou 730070, China*

Correspondence should be addressed to Zhanjun Hao; zhanjunhao@126.com

Received 17 October 2018; Accepted 14 February 2019; Published 10 March 2019

Academic Editor: Michele Garetto

The detection of target events is an important research area in the field of wireless sensor networks (WSNs). In recent years, many researchers have discussed the problem of WSN target coverage in a two-dimensional (2D) coordinate system. However, the target detection problem in a 3D coordinate system has not been investigated extensively, and it is difficult to improve the network coverage ratio while ensuring reliable performance of WSN. In addition, sensor nodes that are initially deployed randomly cannot achieve accurate target coverage in practice. Moreover, it is necessary to consider the energy consumption factor owing to the limited energy of the sensor node itself. Hence, with the objective of addressing the target event coverage problem of WSNs in 3D space applications, this paper proposes a target detection coverage algorithm based on 3D-Voronoi partitioning for WSNs (3D-VPCA) in order to ensure reliable performance of the entire network. First, we extend Voronoi division based on the 2D plane, which allows 3D-Voronoi partitioning of sensor nodes in 3D regions. Then, it is optimized according to the 3D-Voronoi neighbouring node partitioning characteristics and combined with the improved algorithm. Next, we set the priority coverage mechanism and introduce the correlation force between the target point and the sensor node in the algorithm, so that the sensor node can move to the target position for accurate coverage. Finally, we carry out related simulation experiments to evaluate the performance and accuracy of the proposed algorithm. The results show that the proposed algorithm can effectively improve the coverage performance of the network while ensuring a high overall coverage ratio.

1. Introduction

A wireless sensor network (WSN) is a multihop ad hoc network consisting of a set of sensor nodes, small devices, etc., which are tasked with monitoring events in the region of interest and transmitting the collected data to the data centre for processing [1, 2]. The sensor nodes can be autonomous or stationary. Thus, we can organize the movement of the sensor nodes through self-deployment (e.g., by humans or mobile robots) [1]. In recent years, WSNs have witnessed many applications, such as target detection [3], target location [4], healthcare monitoring [5], and data collection [6]. Research on WSNs coverage is mainly classified into three branches: area coverage, barrier coverage, and target event coverage. Among them, target event coverage has long been an important research branch. We can deploy sensor nodes in the monitoring area to sense whether there are specific targets or events in practice. Hence, the main issues that we need to consider in the process of target coverage are as follows:

(1) How to effectively improve the coverage and node utilization rate of the entire network

(2) How to guarantee high coverage ratio and connectivity of the network, reduce the energy consumption of the nodes, and prolong the network life time

(3) How to design algorithms or methods to ensure that the experimental environment is closer to a realistic 3D environment

In this study, we mainly investigate the target detection coverage of WSNs in 3D space. Previous studies on target coverage detection have achieved significant progress in terms of the theory, method, and experiment of using a 2D

plane coordinate system to solve the 3D target coverage problem in a real-world environment, as discussed in the literature [7–9]. However, relatively few studies have investigated the coverage of WSNs directly applied to a 3D coordinate system. On the one hand, it is because the research difficulty increases with the dimension. On the other hand, the coverage problem of sensor nodes in a realistic 3D environment is often affected by the surrounding complex terrain and adverse weather conditions. In a real-world environment, sensor nodes are usually randomly deployed in the monitoring area, resulting in low utilization of the nodes. Hence, how to reduce the energy consumption of the sensor nodes and improve the coverage ratio of the network and the reliability of the algorithm are critical factors to be considered. In the literature [3], a more realistic signal detection model has been developed to obtain information on the target event and make the final decision by using a probabilistic decision model. Furthermore, a probabilistic detection algorithm [3] has been proposed to exploit the local measurements collected by the sensor nodes and improve the utilization rate of the nodes. In addition, a tracking framework based on Voronoi Tessellations has been proposed [10], whereby two mobility models are designed to control the coverage degree according to the existence of the target. Although this method can effectively monitor target events and discover redundant nodes, it is not suitable for realistic 3D conditions. A target-based Voronoi greedy algorithm (TV-Greedy) has been proposed [11] to find approximate optional solutions in order to improve the coverage quality of the network nodes while maximizing the effective energy consumption of the nodes. Although the TV-Greedy algorithm can effectively improve the robustness of the network, it is difficult to apply it to a 3D coordinate system. Thus, it is difficult to directly apply the traditional WSN coverage methods for a 2D coordinate system to a 3D coordinate system. The environment and position information of the target point in 3D space are more complicated. Hence, we need to redesign the deployment scheme of the sensor nodes in 3D space and propose relevant algorithms to achieve effective target coverage and a high coverage ratio of the network.

In summary, this study first designs and extends the traditional Voronoi diagram partitioning method and applies it to a 3D coordinate system, i.e., the 3D-Voronoi partitioning method is designed to solve the 3D space problem. Furthermore, the specific partitioning method is presented. Second, we propose an improved mobile algorithm to improve the detection effect and coverage ratio of the sensor network while addressing the omission problem of the target event to be monitored in the given space. In addition, we experimentally evaluate the network energy consumption as well as the accuracy and feasibility of the proposed algorithm in order to further reduce the network energy consumption. Moreover, we design a priority coverage mechanism and use the improved virtual force algorithm to achieve sensor node movement. Finally, we conduct experimental simulations and comparative analysis to further analyse the effectiveness of the algorithm. The main contributions of this article are as follows:

(1) To the best of our knowledge, this is the first study to propose the application of the 3D-Voronoi partitioning method to target detection coverage of 3D WSNs.

(2) We propose an improved 3D-Voronoi algorithm to ensure a high coverage ratio of the WSN on the basis of the energy consumption and connectivity factors of the network.

(3) We optimize the traditional virtual force algorithm (VFA) to suit new environments and practical conditions. Furthermore, we conduct a full theoretical analysis of the algorithm and compare it with two other algorithms to verify its effectiveness and accuracy.

The remainder of this paper is organized as follows. Section 2 reviews the research progress and related studies on WSNs in recent years. Section 3 describes the design of the network model and the 3D-Voronoi partitioning model. In addition, it states the related definitions employed in this paper. Section 4 discusses how the related algorithms are designed and improved. Furthermore, it outlines the design steps of 3D-VPCA algorithm. Section 5 presents the theoretical analysis of the network coverage ratio and energy consumption of the proposed algorithm. Section 6 describes the simulations and experiments performed to compare the proposed algorithm with two other algorithms. Finally, Section 7 states the conclusions and briefly explores directions for future work.

2. Related Works

In recent years, many studies and analyses have been carried out using the Voronoi plane to divide target events and sensor nodes. In particular, the optimal deployment of sensor networks is currently a research hotspot. Under some special circumstances, sensor nodes are often randomly distributed in a region. Optimizing the cost and utilization of limited resources has become the focus of current research. For example, in [12], distributed self-deployment schemes of mobile sensors have been proposed to solve the problem of efficiently deploying wireless sensor nodes. The authors designed two schemes by using a Voronoi diagram and a centroid, namely, Centroid (i.e., based on centroid scheme) and Dual-Centroid (i.e., based on dual-centroid scheme), to improve the speed and efficiency of node coverage holes. In [13], the authors proposed a deployment method for nodes in large-scale and high-density WSNs on the basis of centroid Voronoi Tessellation (CVT), which approximates the solution through the geometry of random points. Furthermore, the authors proposed a deployment plan based on the given characteristics of the study area in order to achieve near-ideal deployment. In some cases, owing to the initial random distribution of sensor nodes, there are coverage holes in the monitoring area. Hence, it is necessary to consider the survival time and cost of the network. Therefore, a two-phase coverage enhancing algorithm for hybrid WSNs was proposed in [14]. In the first phase, the authors used a differential evolution algorithm to compute the

candidate's target point positions in the mobile sensor nodes in order to improve the coverage ratio. In the second phase, they used an optimization scheme for the candidate's target positions calculated in the first phase in order to reduce the moving distance of the mobile sensors. Finally, accurate filling of the coverage holes was achieved. Furthermore, the power supply module of the sensor node is a dry battery with limited energy, which can supply power only for a certain period of time. Hence, the energy consumption of nodes is a key research consideration. In [15], the authors discussed the energy consumption issue of target detection in WSNs and established a framework for evaluating performance indicators to analyse the performance of sensor networks as well as the quality of service. In [16], the author discussed the key issues of how to balance the target detection quality and lifetime of WSNs, and two target-monitoring schemes were proposed. One exploits the residual energy in the network and uses the adjustable sensing frequency in different regions to improve the monitoring quality. The other provides a method for calculating the optimal frequency value of the nodes with residual energy. Although the network energy consumption and monitoring quality factors have been considered in [15, 16], they have not been comprehensively considered or verified for a 3D coordinate system. Furthermore, the algorithms and methods proposed in the abovementioned studies are based on a 2D coordinate system, whereas actual scenarios are tested and verified in a 3D environment. Hence, some coverage methods for realistic 3D environments have also been proposed. For example, in [17], the authors proposed a distributed algorithm for mobile robotic sensors to allow self-deployment of sensor nodes in a 3D environment in order to achieve complete blanket coverage. This algorithm aims to achieve full coverage of the network while considering issues such as obstacles in the environment, and it minimizes the number of sensor nodes and mobile energy consumption. In [18], the authors pointed out that traditional probability coverage problems of WSNs mainly focus on 2D space. However, most practical applications of WSNs are in 3D space. Hence, in [18], the authors introduced a probability model of 3D WSNs and proposed a scheduling algorithm (PMCCA) that uses Voronoi division to control the scheduling of the probability model nodes in the target region. In [19], a 3D space deployment algorithm was proposed for continuous target tracking to overcome the dispersion problem of the traditional virtual force algorithm as well as the short-time tracking problem in the process of target tracking. In addition, the authors combined the internode force, the obstacle repulsive force, and the attractive force between the monitored-path and the tracking target into a virtual resultant force, so that the coverage of the target path is more continuous and sustained. Compared with the traditional virtual force algorithm, the abovementioned algorithm improves the effective time of the continuous target-tracking process and shortens the time of losing targets. In general, the algorithm or method proposed in [17–19] achieves effective detection of targets in 3D conditions. By contrast, our scheme is more direct and effective, and we have made more comprehensive considerations. In [20], the complete coverage problem of mobile sensor networks in a 3D environment was studied. The authors proposed a decentralized random algorithm to drive a group of mobile sensors on the vertices of a truncated octahedral grid for complete coverage of a bounded 3D area. However, the node utilization is not high, and this approach is not suitable for target event monitoring. In [21], a new network coverage and optimization control strategy based on a genetic algorithm was proposed to solve the deterministic coverage problem of sensor nodes. In addition, the author reduced the 3D coordinate system to a 2D plane in order to determine the fitness function of the relevant solution, and they used iteration to find the optimal solution. However, the abovementioned approach is based on the conditions of node deterministic deployment and is not applicable to the random deployment conditions considered in this paper.

In early coverage research on 2D-Voronoi partitioning, a distributed self-deployment protocol for mobile sensors was proposed [22] to calculate the correct location of the mobile node in order to solve the coverage vulnerability problem. Furthermore, the author considered the transition problem of nodes in the coverage area from dense to sparse and designed three sensor node mobility assistance algorithms. Experiments showed that these algorithms can achieve a higher coverage ratio in a short time with limited moving distance. Owing to the random deployment of a large number of sensor nodes in a real environment, the network degree of coverage is not high. In [23], a mobile sensor network coverage optimization algorithm based on virtual force perturbation and cuckoo search (VF-CS) was proposed. The Voronoi diagram was divided into sensor nodes to form their respective Thiessen polygons; then, a virtual force between the polygon vertices and the neighbour nodes was introduced as the perturbation factor of the node position update. Finally, the cuckoo algorithm was used to optimize the mobile coverage. In [24], to solve the problem of coverage holes in static WSNs, the authors proposed a triangle patch method to enhance the mobile node's ability to repair coverage holes. Finally, the authors used the algorithm auxiliary information provided by the coverage edge nodes to move the nodes to the best candidate location. In [25], to reduce the cost of the K-coverage sleep-scheduling algorithm and ensure effective monitoring by the nodes, the prescheduling-based K-coverage group scheduling (PSKGS) and self-organized K-coverage scheduling (SKS) algorithm were proposed. Finally, the authors concluded that the PSKGS algorithm improves the monitoring quality and network lifetime through simulation experiments, while the SKS algorithm reduces the computational and communication costs of the nodes. Obviously, the research based on 2D-Voronoi algorithms has shown better results, but it can rarely be applied to a 3D coordinate system. Therefore, this paper extends traditional Voronoi studies [22–24] to 3D wireless sensor network target detection coverage.

In the subsequent experiments, we compare the proposed algorithm with the CSA algorithm and the RA algorithm. Although the three algorithms can achieve effective detection, the coverage ratio of our algorithm is shown to be optimal.

3. Network Coverage and Voronoi Partitioning Method

3.1. Network Coverage Model. This paper studies the problem of WSN target detection coverage in a 3D environment. Therefore, we assume that the sensing model of the sensor node is a spherical coverage area with node coordinate $s_i(x_i, y_i, z_i)$ as the centre and the sensing range R_s as the radius. Initially, it is assumed that n sensor nodes are randomly scattered in a target area of size $L \times L \times L$, and the set of nodes is $n_i\{n_1, n_2, \cdots, n_i\}$. Owing to the random deployment of nodes in the initial stage, various problems, such as uneven distribution of sensor nodes, excessive energy consumption of nodes, and repeated coverage of some target points, may occur. Thus, the utilization of the node is reduced. Furthermore, some target points may be missing and not covered. As shown in Figure 1 below, some target points are in the coverage area of the nodes, and some are not covered by the nodes. Among them, the three black mesh spheres represent the coverage of three nodes, and the small black dots represent randomly distributed target point events. Furthermore, the node sensing model shown in Figure 2 represents the relationship between the communication radius of the node and its sensing radius. The proof in [26] shows that the connectivity between network nodes can be guaranteed when the communication radius of the node is at least two times the sensing radius, i.e., $R_c \geq 2R_s$. Figure 2 shows the sensing model of the node, where the small balls represent R_s as the sensing range of the node o, and the large balls represent the communication range with R_c as the node o.

First, we make the following assumptions before studying the 3D WSN coverage algorithm based on 3D-Voronoi partitioning:

(i) The sensing radius R_s and communication radius R_c of the sensor node are isomorphic, and $R_c = 2R_s$

(ii) The sensor nodes can be moved in space

(iii) The sensor nodes can capture their own location information through some technical means

For a more intuitive follow-up analysis and discussion of this article, we introduce the following definitions to better describe the problem.

Definition 1. neighbour node. The communication range of the sensor nodes s_i is a sensing sphere with R_c as the communication radius. When the Euclidean distance $d(i, j)$ between the two sensor nodes i and j in space satisfies $d(i, j) \leq R_c$, the two nodes are said to be neighbour nodes. Thus, the spheres of the sensing range between the two nodes will intersect or be tangent [27].

Definition 2. network coverage ratio. In this paper, the probability sensing model can be used to determine the probability that any point $p(x, y, z)$ in space is covered by node s_i as follows:

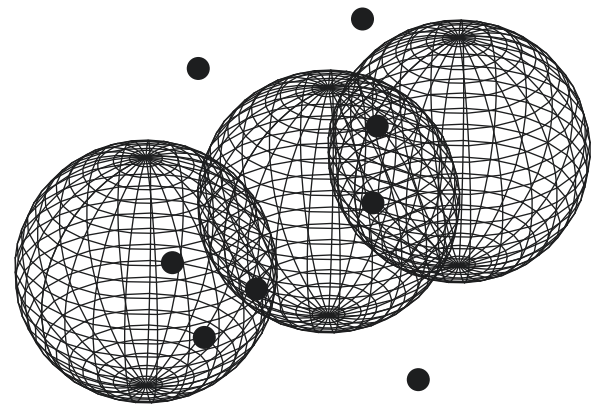

Figure 1: Node coverage model.

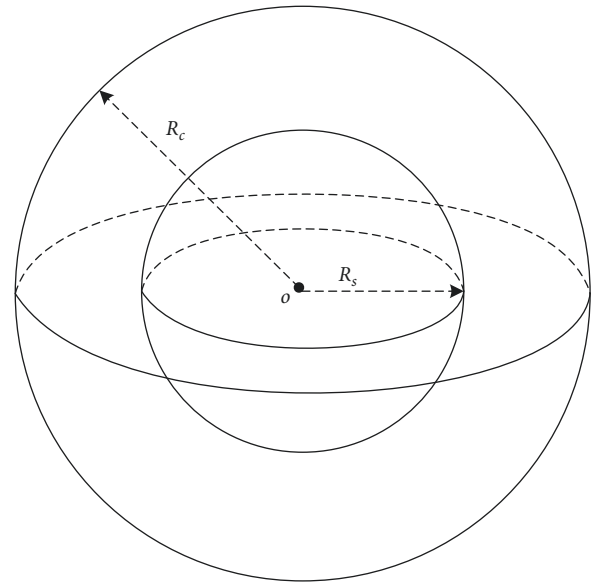

Figure 2: Node sensing model.

$$S_p(s_i) = \begin{cases} 1, & d(s_i, p) < r_{\min}, \\ e^{-ad^{\lambda}}, & r_{\min} \leq d(s_i, p) \leq R_s, \\ 0, & d(s_i, p) > R_s, \end{cases} \quad (1)$$

where $d(s_i, p)$ represents the Euclidean distance between points $p(x, y, z)$ and s_i, which can be calculated by Equation (2); λ is the sensing attenuation factor, which is the physical property of the nodes; and $r_{\min}$ is a value between 0 and r_s, which is based on multiple experiments. Equation (1) indicates that when the distance satisfies $d(s_i, p) < r_{\min}$, strong detection is achieved, and $r_{\min} \leq d(s_i, p) \leq R_s$ indicates weak detection.

$$d(s_i, p) = \sqrt{(x - x_i)^2 + (y - y_i)^2 + (z - z_i)^2}. \quad (2)$$

Suppose that there are n nodes $s_1, s_2, \cdots, s_n$ in the network, and their coverage ratios to a point p are $s_p(s_1), s_p(s_2), \cdots, s_p(s_n)$, respectively. Then, the coverage ratio of point p in the network is

$$s_p(A) = 1 - \prod_{i=1}^{n}\left(1 - s_p(s_i)\right), \tag{3}$$

where p represents the target point to be detected. If k target points are taken in the network and the coverage ratios of these target points is averaged, the entire network coverage ratio of the network can be obtained as follows:

$$S(A) = \frac{1}{k}\sum_{i=1}^{k} s_i(A). \tag{4}$$

It should be noted that $S(A)$ is a statistical value in the actual environment. When the value of k is sufficiently large, the statistical and theoretical values will be infinitely close.

3.2. 3D-Voronoi Model

3.2.1. Voronoi Principle. In early research on the 2D-Voronoi WSN coverage model, the initial nodes were randomly distributed in a 2D plane. Hence, a part of the same area or a single target point event may be covered by multiple sensor nodes, resulting in considerable node redundancy. To overcome this problem, many related studies have reduced the nodes in 3D space to a 2D plane and divided them using a Voronoi diagram. As shown in Figure 3, given a set of sensor nodes $s_i = \{s_1, s_2, \cdots, s_n\}$, the bounded plane is divided into n polygonal cells $F_i (i = 1, 2, \cdots, n)$. Therefore, the cell $F_n = \{F_1, F_2, \cdots, F_n\}$ of each node contains exactly one of the sensor nodes s_i, and s_i is called the F_i divided generation node [28]. Furthermore, according to the partitioning property of the Voronoi diagram, the distance from any point p in each unit F_i to s_i in the unit is shorter than the distance between the point p and the neighbour nodes around s_i.

Hence, the definition of the division of the 2D-Voronoi diagram partition satisfies the following equation:

$$S_i = \bigcap_{i\neq j, j=1}^{n} \{p \mid D(s_i, p) \le D(s_j, p),\ j = \{1, 2, \cdots, n-1\}, \forall j \neq i\}, \tag{5}$$

where $p(x, y)$ represents the coordinates of any point in the monitoring area. The Euclidean distance from node s_i or s_j to point p is

$$D(s_i, p) = \sqrt{(x_i - x)^2 + (y_i - y)^2}. \tag{6}$$

As shown in Figure 3, there are 100 sensor nodes distributed in the plane. According to the definition of the Voronoi diagram, each Voronoi unit contains its own unique node. As shown in Figure 4, the red circle represents the coverage of each node. Assuming that the sensing radius of each node is R_s, after the sensor nodes in the plane undergo Voronoi division, the coverage area of each node is πR^2.

3.2.2. 3D-Voronoi Partition Method. After reviewing the related 2D-Voronoi research in the previous section, we extend it to a 3D space coordinate system for division. First, the 3D space is divided into Voronoi polyhedron 'V-body' units, where each 'V-body' is an irregular multifaceted closed convex body. We define the above division as 3D-Voronoi partitioning. The 3D-Voronoi partition is defined as follows: assuming a set of n nodes $s_n = \{s_1, s_2, \cdots, s_n\}$ in the 3D $L \times L \times L$ space, partition a 3D L^3 space into n 'V-body' units $V_n = \{V_1, V_2, \cdots, V_n\}$. The unit $V_i (i = 1, 2, \cdots, n)$ contains a unique node s_i; then, s_i is called the generation point of V_i. Therefore, the distance from any point p to node s_i inside a certain unit body V_i is shorter than the distance between p and other s_j nodes. Thus, the definition satisfies the following equation

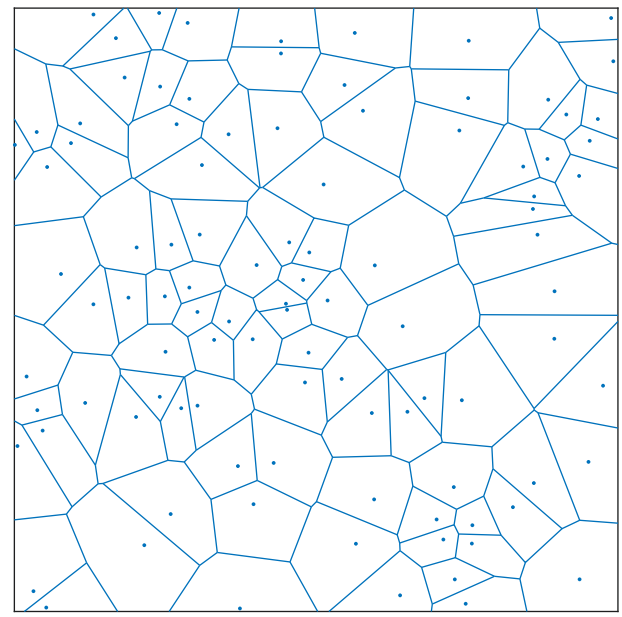

Figure 3: 2D-Voronoi diagram.

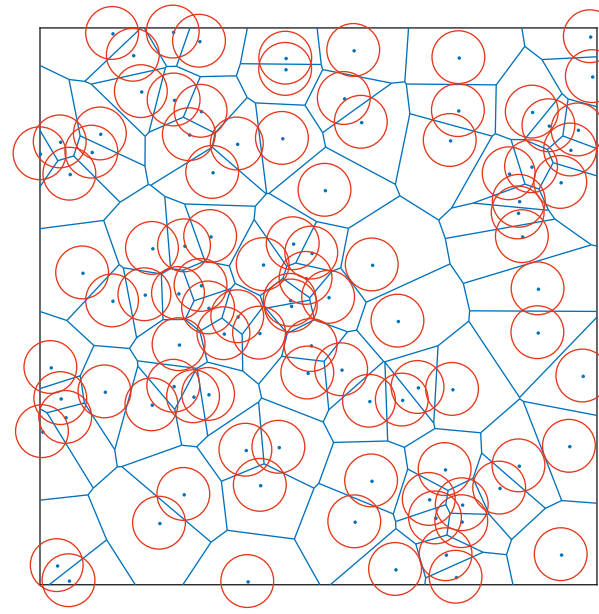

Figure 4: 2D-Voronoi node coverage.

$$Q(V,V_i) = \{V_i \in V \mid d(p,(V,s_i)) \le d\left(p,\left(V,s_j\right)\right), \quad j = \{1,2,\cdots,n-1\}, \forall j \ne i\}. \tag{7}$$

The Euclidean distance from node $s_i(x_i, y_i, z_i)$ in the V-body to any point $p(x, y, z)$ in space is

$$d(s_i,p) = \sqrt{(x_i-x)^2 + (y_i-y)^2 + (z_i-z)^2}. \tag{8}$$

It can be concluded from the aforementioned results that the 2D-Voronoi diagram is a continuous polygon composed of a set of vertical bisectors connecting the straight lines of two neighbouring points, and the set of continuous polygons is seamless and unique. Therefore, each of the division units constituting the 3D-Voronoi diagram is changed from a polygon of a 2D plane to a collection of 3D polyhedra $V_i\{V_1, V_2, \cdots, V_n\}$. As shown in Figure 5(a), we divide the 3D 100 m^3 cube space. It can be seen that the cube surface is composed of many irregular polygons similar to 2D planes. Furthermore, the size of the partition density is determined by the value of the node. Further internal division can yield a 3D-Voronoi division shape as shown in Figure 5(b). The small black dots in the figure represent nodes s_i, and each polyhedron having a different shape indicates that the cube is divided into Voronoi polyhedral units of different sizes. In addition, it can be seen that each V-body unit contains only one node (e.g., black dots as shown in Figure 5(b)). Thus, the number of nodes s_i is the same as the number of V-body units after division, i.e., $(\mathrm{NUM}_{s_i} = \mathrm{NUM}_{V_i}, \quad i = (1,2,\cdots,n))$. As shown in Figure 5(c), increasing the number of nodes can result in more V-body units with smaller volumes, making the divided V-bodies denser. Second, according to the definition of Voronoi partition, the Einstein distance from node s_i in the interior of the V-body to an arbitrary point in V-body is shorter than the distance from the node s_i to a neighbour node or other nodes. Therefore, this paper first uses this important property to divide and study the coverage problem of 3D space.

4. Algorithm Design and Steps

In this paper, we mainly study the coverage detection problem of target events in 3D space. Initially, the sensor nodes are randomly deployed, but there may be uncertainties in the target point events. Hence, we first assume that the position information of the target points is known and the position coordinates are determined experimentally. Second, the nodes can also know their location information after random deployment. Furthermore, the nodes have the same sensing radius and communication radius, i.e., the nodes in the WSN are isomorphic. Initially, the nodes can be separated into independent and unique V-body units by means of 3D-Voronoi partitioning after random deployment. However, this paper does not use the Voronoi method to divide the target event; instead, it uses the 3D-Voronoi method to divide the sensor nodes. According to the Voronoi property, we first consider the coverage problem of the sensor node in the V-body unit. For target points that are not in the range of node perception, we need to design related algorithms to implement mobile node coverage.

4.1. Definition of Virtual Force. In the WSN coverage, the virtual force algorithm (VFA), whereby randomly deploying nodes in the monitoring environment is redeployed by different virtual field forces, has been widely applied. The virtual force was first derived from physics. When the distance between two atoms is extremely small, they develop mutual repulsive forces that separate them. Furthermore, when the distance between the two atoms is extremely large, an attractive force is developed to draw them closer [29]. In this article, we need to redesign the improved virtual force algorithm to solve the following problems:

(i) How to use the 3D-Voronoi partitioning method to divide the nodes and redeploy them to accurately cover the target point events

(ii) How to define the virtual force generated between the nodes and the mutual attraction, repulsive force, and obstacle repulsive force between the various forces

(iii) How to use the improved algorithm to move redundant nodes to cover missing target points in order to improve the coverage ratio

To further improve the coverage ratio and accuracy of the algorithm, we consider how to avoid node energy consumption or node death due to excessive invalid movement. We will describe the algorithm design in detail in the following section.

4.2. Virtual Force Analysis. Owing to the initial random deployment of the nodes, we first use the 3D-Voronoi partitioning method to make the nodes within their respective independent V-body units, and we do not divide the covered target points. First, we consider that the nodes preferentially cover the target points in the respective V-bodies, so the sensor nodes are preferentially set to perform mobile coverage in the V-body units to which they belong. In the improved virtual force algorithm, we assume that the node is subjected to three forces in the 3D region. In the optimization process of the coverage algorithm, each sensor node moves with the total resultant F_A, thereby achieving the balance of the nodes as well as uniform coverage of the target events. Hence, in the monitoring region, we assume that the sensor node is subjected to the gravitational force with the target event represented by F_a, the interaction force between the neighbouring nodes is represented by F_{ij}, and the force of the boundary obstacle and the node in the target region V represented by F_c. Hence, the node is subjected to the total resultant force F_A:

$$F_A = \sum_{j=1, j\ne i}^{n} F_{ij} + F_a + F_c. \tag{9}$$

4.2.1. Interaction between Nodes. To further constrain the traditional 3D virtual force, the node prematurely dies owing to excessive movement of the node distance. Toward this end, we introduce distance thresholds $r_{\min}$, r_b equivalent between nodes, where $r_{\min}$ represents the minimum safe

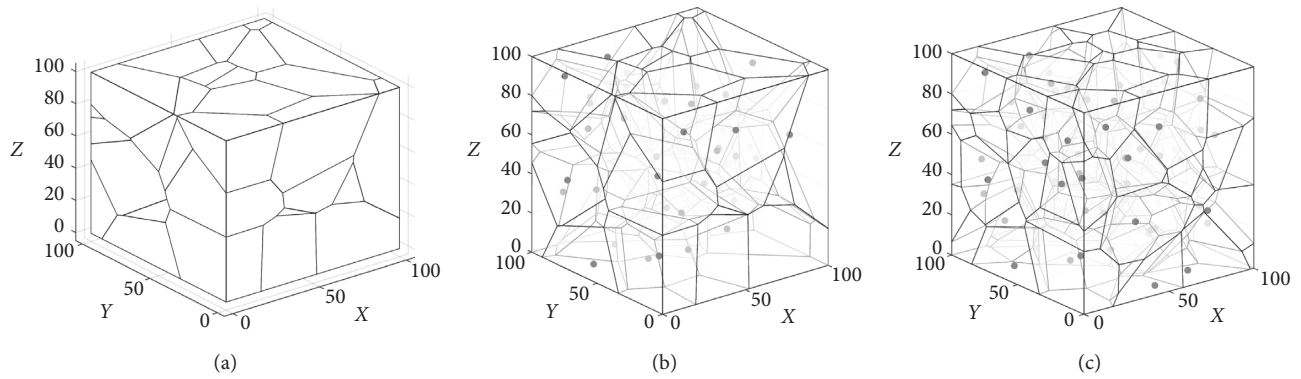

Figure 5: 3D space partition diagram. (a) 3D space surface partition. (b) 3D space sparse partition. (c) 3D space dense partition.

distance of the node and r_b represents the positional distance between the nodes when the resultant force is zero. In [30], the author explained the optimal distance between nodes to ensure the connectivity of the nodes. The equation $d_{ij} = 2r_s$ is used when there are few nodes, and the equation $d_{ij} = \sqrt{3}r_s$ is used when there are many nodes. Therefore, to ensure the connectivity of the nodes, the equation $r_b = d_{ij} = \sqrt{3}r_s$ is used first. Furthermore, the interaction force F_{ij} between the nodes is calculated as follows:

$$F_{ij} = \begin{cases} +\infty, & 0 < d_{ij} \le r_{\min}, \\ \dfrac{k_1 m_i m_j}{d_{ij}^{a_1}}, & r_{\min} < d_{ij} < r_b, \\ 0, & d_{ij} = r_b, \\ \dfrac{-k_2 m_i m_j}{d_{ij}^{a_2}}, & r_b < d_{ij} < R_c, \\ 0, & d_{ij} > r_b, \end{cases} \tag{10}$$

where k_1, k_2, a_1, and a_2 represent gain coefficients; m_i and m_j represent the quality factor of the node (i.e., usually taking the value of 1); and d_{ij} represents the Euclidean distance between node i and node j. When the distance between nodes is between $r_{\min}$ and r_b, the nodes are mutually exclusive. When the distance between nodes is equal to r_b, the node is not affected by any force. When the distance is between r_b and communication radius R_c, the nodes attract each other. When $d_{ij} > R_c$, the force between the nodes disappears.

4.2.2. Gravitational Force of the Target Event on the Node. To enable the randomly deployed nodes to effectively cover the target points within the respective V-body units, we set the target point as the attraction sources with the nodes. It is assumed that the position coordinates of the sensor node and the target point are represented as $s_i(x_i, y_i, z_i)$ and $o_j(x_j, y_j, z_j)$, respectively. If the target point is used as the attraction source of the node, the target event has a gravitational effect on the sensor nodes within a certain range. Therefore, to solve the problem that there may be a target point that does not enter the sensing range of the node, we add the gravitational effect between the target and the node to force the node to move the coverage. The gravitational pull of the target event on the node can be calculated by

$$F_a = \begin{cases} \dfrac{-k_3 m_{p_i} m_j}{d(p_i, j)^{a_e}}, & j \in Q(P), \\ 0, & \text{other}, \end{cases} \tag{11}$$

where k_3, a_e represent the gain coefficient, and $d(p_i, j)$ represents the Euclidean distance from node j to event p_i. Furthermore, m_{p_i}, m_j represent the quality factor of the event p_i and the node j, respectively, and $Q(P)$ represents the gravitational force generated by the event set P in the area of action. When the node is within the gravitational range generated by event set P, the node is attracted to P.

4.2.3. Repulsive Force between Boundary Obstacles and Nodes. The virtual gravity F_a will cause the node to move to the target event. If only the effect of gravity causes a large number of nodes to move to fewer target points, complete and effective coverage cannot be achieved, and the nodes may consume too much energy owing to excessive moving distances. On the contrary, we need to consider the problem of preventing collisions between a node and an obstacle during the movement. Thus, we also need to introduce boundary repulsion to improve the overall coverage while ensuring that the distance between adjacent nodes is in the optimal range. Hence, the boundary repulsion is obtained by the following equation:

$$F_b = \begin{cases} \dfrac{k_4 m_i m_j}{d_{ij}^{a_e}}, & 0 < d_{ij} \le L, \\ 0, & d_{ij} > L, \end{cases} \tag{12}$$

where k_4 and a_b are the gain coefficients, and L is the Euclidean distance between the node i and the obstacle. When

the node and the obstacle are within a certain range, the node will be repelled by the obstacle.

4.3. 3D-VPCA Algorithm. On the basis of the above-mentioned theoretical analysis and algorithm description, we propose a target detection coverage algorithm based on 3D-Voronoi partitioning for 3D WSNs, namely, 3D-VPCA. Initially, sensor nodes are deployed in a 3D area that needs to be monitored. Subsequently, the sensor networks begin to execute the proposed algorithm to perform 3D-Voronoi partitioning and establish communication with each node. At this time, the node first judges the current location information and the energy consumption state and calculates the positional relationship with the neighbour node. Then, the node again judges whether to perform readjustment according to the current location information. If there is a target point that is not covered by the nodes in the V-body unit, the node will be redeployed by the virtual force resultant F_A to move the position to the final ideal coverage. Based on the analysis presented above, the implementation steps and flow of the 3D-VPCA algorithm paper are as follows:

Step 1. n sensor nodes are randomly deployed in the area L to be monitored, and each node first determines the location of each location coordinates and the location information with the neighbour nodes.

Step 2. The 3D-Voronoi method is used to divide the area where the sensor nodes are located, so that each node is in its own V-body unit.

Step 3. To solve the problem of missing the target coverage caused by the traditional virtual force algorithm, the proposed algorithm is divided into three cases. Case 1: The target point is within the coverage of the node. Case 2: There are multiple target points in the V-body, but some of the target points are not within the coverage of the node. Case 3: There may be a situation where the target point is located on the boundary of two neighbour V-bodies.

Step 4. It is judged whether the target event is covered at this time according to the distance relationship of the covered target point to the node. If the number of target points covered is $N_{c_j} \geq 1$, execute step 5; otherwise, execute step 6.

Step 5. Keep the current number of nodes s_k (i.e., k is the number of nodes that cover the target event). Thereafter, the idle node s_f (i.e., $s_f = s_i - s_k$) is preferentially selected for movement.

Step 6. The idle node s_f ($s_f = s_i - s_k$) at this time is checked, and the number of remaining target points N_{c_j} (i.e., $N_{c_j} = N_{o_i} - N_{c_i}$) is calculated, where N_{o_i} is the total number of target points.

Step 7. It is judged whether there are two neighbour boundary nodes, the node of the V-body to which the target point belongs is preferentially moved, and the idle neighbour nodes on both sides of the neighbour boundary.

Step 8. Mobile coverage optimization is performed by the 3D-VPCA algorithm (Algorithm 1), and the idle node s_f is moved to cover the remaining target point c_j by the virtual force resultant F_A of the algorithm.

Step 9. Repeat step 4–8 until all nodes move to reach the optimal position and complete the final coverage.

5. Theoretical Analysis of the Algorithm

5.1. Coverage Rate Analysis. The probability $S_p(s_i, p)$ that the target point set p is covered by the node $s_i(x, y, z)$ can be obtained by the following equation [31]:

$$S_p(s_i, p) = \begin{cases} 1, & d(s_i, p) < r_{\min}, \\ e^{-ad^{\lambda}}, & r_{\min} \leq d(s_i, p) \leq r_s, \\ 0, & d(s_i, p) > r_s, \end{cases} \tag{13}$$

where λ represents the perceived attenuation factor, which is the physical property of the node; and $r_{\min}$ represents a value between 0 and r_s, which is based on multiple experiments. Assuming that there is a certain target event p in 3D WSNs, the Euclidean distance between these events p from any node $s_i(x_j, y_j, z_j)$ deployed in 3D space can be calculated by Equation (2). However, under the action of the virtual force, the node p is moved by the magnitude and direction of the resultant F_A. Thus, there is a difference between the Euclidean distance after the target event s_i and the node p movement and the Euclidean distance before the movement. The equation for the distance after the change is

$$d'(s_i, p) = d(s_i, p) + \mathrm{dir}_p. \tag{14}$$

Finally, Equation (14) minus Equation (2) gives.

$$d'(s_i, p) - d(s_i, p) = \mathrm{dir}_p = \arctan(F_A) \times \frac{2}{\pi} \times \overline{|\mathrm{dir}_{\max}|}, \tag{15}$$

where $\mathrm{dir}_{\max}$ represents the direction vector of the node's moving distance, and its direction is opposite to dir_p. Therefore, $\arctan(F_A) \times (2/\pi) \times \overline{|\mathrm{dir}_{\max}|}$ is a number less than zero; then, $d'(s_i, p) < d(s_i, p)$ can be derived. Therefore, the probability that $d'(s_i, p)$ is smaller than R_s will be greater, which indicates that the probability of the node covering the target event is higher under the action of the 3D-VPCA algorithm. Finally, it can be concluded from the above theoretical proof that the algorithm improves the coverage ratio of the overall network.

5.2. Energy Consumption Analysis. In sensor networks, each node is mainly responsible for sensing the surrounding environment and transmitting the sensing data. Therefore, in this study, the node's energy consumption includes sensing and communication [32, 33]. The WSNs in this study have two aspects of the main energy consumption under the action of the improved virtual force algorithm; the energy consumption per unit of communication between the nodes is denoted by e_c, and the mobile energy consumption of the node per unit distance in any direction is denoted by e_d. Furthermore, E_c represents the mobile energy

The pseudo code of the 3D-VPCA algorithm is given as follow:
(1) s_i: The area of the sensor nodes
(2) o_i: The area of the target nodes
(3) **Input:** The total number of sensor nodes n and the perceived radius of the nodes R_s
(4) **Output:** Location coordinates and network coverage $S(A)$
(5) **Initialization:** Divide the three-dimensional Voronoi 'V-body' unit v_i
(6) Num = n
(7) maxiter = 100 Set the maximum number of iterations
(8) max_step = 0~10 Set the maximum moving step size of the node
(9) $A = x * \text{rand}(n,1) \pm x\text{max}$
(10) $B = y * \text{rand}(n,1) \pm y\text{max}$
(11) $C = z * \text{rand}(n,1) \pm z\text{max}$
(12) $S_i\ (X, Y, Z) = (A,B,C)$ Randomly generated n nodes in the area
(13) Dividing 'V-bodies' $\in v_i$, $v_i = (v_1, v_2, \cdots, v_n)$
(14) **while** $i \le$ Num **do**
(15) **if** $d_{ij} \le R_s$ **then**
(16) save the current nodes s_k and 'V-body' unit v_k
(17) **else**
(18) select the free nodes $\xrightarrow[s_f(s_f=s_i-s_k)]{}$ as coverage s_i
(19) **if** $d_{ij} > R_S$ **&&** $N_{c_j} \ne 0$ **then**
(20) calculate the total virtual force $F_A = \sum_{j=1, j\ne i}^{n} F_{ij} + F_a + F_c$
(21) move $s_f \longrightarrow N_{c_i}$
(22) **else**
(23) move $s_f \longrightarrow$ boundary nodes s_L
(24) **end if**
(25) **end if**
(26) **end if**

Algorithm 1: 3D-Voronoi partition coverage algorithm (3D-VPCA).

consumption of all the nodes in the entire network, and E_d represents the total communication energy consumption of all the nodes in the entire network. Thus, the total energy consumption E of the entire network is

$$E = E_d + E_c = \sum_{i=1}^{n} \sum_{\forall \text{dir}} \left| e_d \times \text{dir}_i \right| + \sum_{i=1}^{n} \left| e_c \times d^2 \right|, \tag{16}$$

where n represents the number of working nodes in the network, and $|\text{dir}_i|$ represents the moving distance of node i in any direction. In addition, $\sum_{\forall \text{dir}} |\text{dir}_i|$ represents the sum of the moving distance of node i in any direction and d represents the communication distance between the nodes in the entire network. Hence, dir_i can be calculated as

$$\text{dir}_i = \arctan F_A \times \frac{2}{\pi} \times \text{dir}_{\max}, \tag{17}$$

where $\text{dir}_{\max}$ represents the maximum distance that the node can move, i.e., the node movement range is $[0, \text{dir}_{\max}]$. Equation (17) is substituted in Equation (16) to give

$$E = \sum_{i=1}^{n} \sum_{\forall \text{dir}} \left| e_d \times \arctan F_A \times \frac{2}{\pi} \times \text{dir}_{\max} \right| + \sum_{i=1}^{n} \left| e_c \times d^2 \right|. \tag{18}$$

It is assumed that the total number of nodes n in the WSNs is constant, and the virtual force-based 3D coverage algorithm does not use the 3D-VPCA algorithm. Thus, the equation for the overall network consumption E' under the action of the virtual force algorithm is

$$\begin{aligned} E' &= \sum_{i=1}^{n} \sum_{\forall \text{dir}'} \left| e_d \times \text{dir}_i' \right| + \sum_{i=1}^{n} \left| e_c \times d^2 \right| \\ &= \sum_{i=1}^{n} \sum_{\forall \text{dir}'} \left| e_d \times \arctan F_i \times \frac{2}{\pi} \times \text{dir}_{\max}' \right| + \sum_{i=1}^{n} \left| e_c \times d^2 \right|. \end{aligned} \tag{19}$$

The total network energy consumption under the algorithm proposed in this paper is compared with that under the action of the VFA-3D algorithm. Equation (18) minus Equation (19) yields

$$\begin{aligned} E - E' = &\sum_{i=1}^{n} \sum_{\forall \text{dir}} \left| e_d \times \arctan F_A \times \frac{2}{\pi} \times \text{dir}_{\max} \right| \\ &- \sum_{i=1}^{n} \sum_{\forall \text{dir}'} \left| e_d \times \arctan F_i \times \frac{2}{\pi} \times \text{dir}_{\max}' \right|. \end{aligned} \tag{20}$$

The total node movement distance under the action of the algorithm is smaller than the total node movement distance under the 3D-VPCA algorithm, i.e., $\sum_{\forall \text{dir}} |\text{dir}_i| < \sum_{\forall \text{dir}'} |\text{dir}_i'|$. Therefore, $E - E' < 0$ can be derived, i.e., $E < E'$. Finally, the energy analysis presented above shows that the 3D-VPCA algorithm can effectively reduce the overall mobile energy consumption of the nodes in the network.

6. Experiment Simulation and Results

6.1. Simulation Environment and Parameter Settings. This study used MATLAB (2015b) software for the simulation

experiments. To verify the algorithm as well as the simulation results and performance, the 3D-VPCA algorithm was compared with other two algorithms. Initially, we randomly deployed the sensor nodes in a 100 m^3 cube monitoring space, in which the detection experiments were performed on the target points for the deployment. To improve the reliability of the experiments, we initially chose to deploy 50 nodes. According to [30], when the node deployment is low, the optimal distance of the node is selected to be $R_c = 2R_s$ in order to ensure the connectivity of the network. We assumed that the target event can be covered by the node, but we considered the possibility of poor network connectivity. Hence, we set up 25 target points to ensure higher coverage while ensuring better network connectivity. Similarly, when the number of nodes was increased to 100, we used the network connectivity optimal distance given by $R_c = \sqrt{3}R_s$ when there were many nodes [30]. Therefore, we chose to deploy 58 target points, i.e., $100/\sqrt{3} \approx 57.74$. The simulation parameters used in the experiment are listed in Table 1.

6.2. Experimental Results and Simulation Diagram. First, we performed the following two sets of simulation experiments, as shown in Figures 6 and 7. As shown in Figure 6(a), the blue sphere represents the sensing range of the sensor node. In the first set of experiments shown in Figure 6(a), 50 sensor nodes were initially deployed in the space of the 100 m^3. In the operation of the 3D-VPCA algorithm, the 3D-Voronoi partitioning method is first used to divide the space of 100 m^3 size into 50 differently shaped and unique V-body units according to the number of nodes. Furthermore, each node s_i is located in the respective unit v_i as shown in Figure 6(b). As shown in Figure 6(c), the red dot represents the target point event to be covered; the blue sphere represents the node that the algorithm moves to adjust to cover the target point. The black sphere represents the sensor node whose target point is not within the sensing range of the node, and it is moved and adjusted to achieve coverage under the action of the algorithm. The following conclusions were drawn from the first set of experiments. When the position coordinates of 25 target points are known, the node coverage to the target point is first preserved under the adjustment of the algorithm. When the target point is not within the coverage of the node, the algorithm selects the node to move for adjustment.

To further verify the adaptability of the algorithm, we performed the second set of experiments as shown in Figure 7. As shown in Figure 7(a), when we increased the number of sensor nodes to 100, we also selected the number of target points to be 58. It can be seen from Figure 7(a) that the sensor nodes are more evenly distributed and dispersed in the space when the number of nodes increases. As shown in Figure 7(b), the number of V-body units divided by the algorithm gradually increases with the number of nodes, and the volume of the V-body units gradually decreases. Hence, the probability that the target point is covered by the node increases according to the Voronoi partitioning property. As shown in Figure 7(c), the number of nodes that need to move increases with the number of target points and nodes.

6.3. Algorithm Analysis and Contrast Experiment. To further verify the accuracy of the experiment, we compared the 3D-VPCA algorithm in this paper with the cuckoo search algorithm (CSA) [34] and the random algorithm (Random Algorithm). Initially, we deployed the nodes in a cube space of size 100 m^3 meters. In the experiment groups 3 and 4, we set the number of target points as 40 and 100 for comparison and then verified the coverage ratio change relationship of the three algorithms under different numbers of nodes by changing the number of sensor nodes. As shown in Figure 8, the number of target points to be monitored was set to 40. The coverage ratio of the three algorithms was compared by verifying the number of different nodes. It can be seen from Figure 8 that the CSA algorithm has a higher coverage ratio than the RA algorithm under the same target number and the same number of nodes. Hence, the coverage ratio of the 3D-VPCA algorithm is significantly better than that of the RA algorithm under the same conditions. When the number of nodes is between 10 and 15, the coverage ratio of the 3D-VPCA algorithm is not as high as that of the CSA algorithm. However, the coverage ratio of the 3D-VPCA algorithm in this paper is significantly improved and full coverage (i.e., the coverage rate is 1) is achieved first under the condition that the number of nodes is greater than 20. Hence, it is concluded from Experiment 3 that the algorithm is more suitable under a large number of nodes, and it can achieve a higher coverage ratio.

In Experiment 4, we increased the number of target points to 100, as shown in Figure 9. Experiment 4 mainly verifies the change in the coverage ratio of the 3D-VPCA, CSA, and RA algorithms when taking different numbers of nodes. When the number of sensor nodes is small and the number of target events is large (as shown in Figures 8 and 9, when the number of sensor nodes is in the range of 0–10), the coverage rate of the three algorithms under the same conditions is significantly lower than that in Experiment 3. Thus, it can be seen that the proposed algorithm has obvious advantages over the RA algorithm under the same conditions. When the number of sensor nodes is less than 20, the coverage ratio of the CSA algorithm is better than the coverage ratio of the proposed algorithm. However, when the number of nodes increases, the 3D-VPCA algorithm is significantly improved and superior to the CSA and RA algorithms. Therefore, it is further illustrated by Experiment 3 and Experiment 4 that the 3D-VPCA algorithm is advantageous under a large number of nodes.

To verify the changes in the various indicators of the three algorithms when changing the target number, we compare the results shown in Tables 2 and 3. In Table 2, we set the number of nodes to 30. In Table 3, we set the number of nodes to 35. Among them, Min and Max represent the minimum and maximum target points covered by the nodes under the same conditions. Furthermore, Avg (%) represents the average ratio of the three algorithms under the same conditions. Finally, we compare the various indicators of the three algorithms.

It can be seen from Tables 2 and 3 that the Min, Max, and Avg (%) indicators of the 3D-VPCA algorithm are significantly higher than those of the other two algorithms under

Table 1: Parameter settings.

Parameter name	Parameter value
Simulation area size L	100 m^3
Total number of targets No_i	25/58
Number of nodes n	50/100
Sensing radius R_s	0~70
Node moving unit distance	30 J
Energy consumption Dir_E	
r_{min}	$R_s \times (5\% \sim 10\%)$
α	0.5
β	0.5

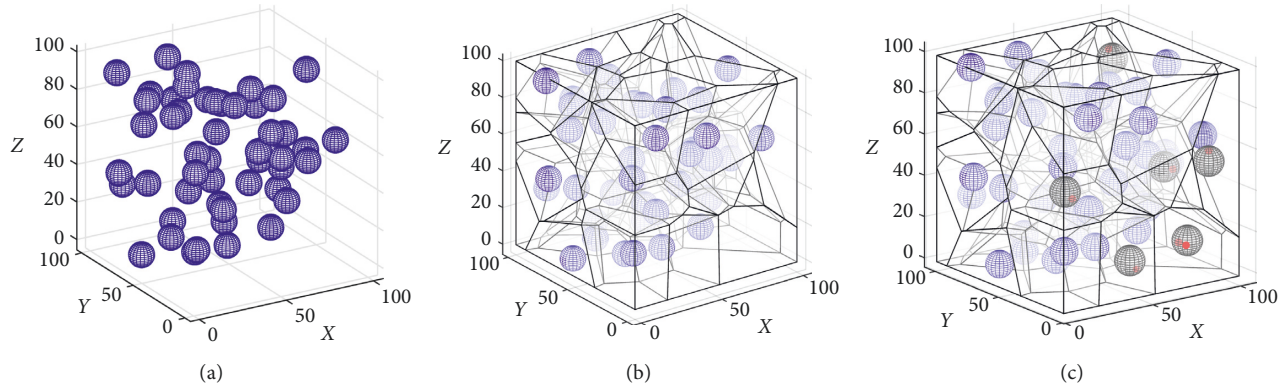

Figure 6: First group simulation experiment diagram. (a) Initial node deployment diagram. (b) Experimental simulation process diagram. (c) Experimental simulation result diagram.

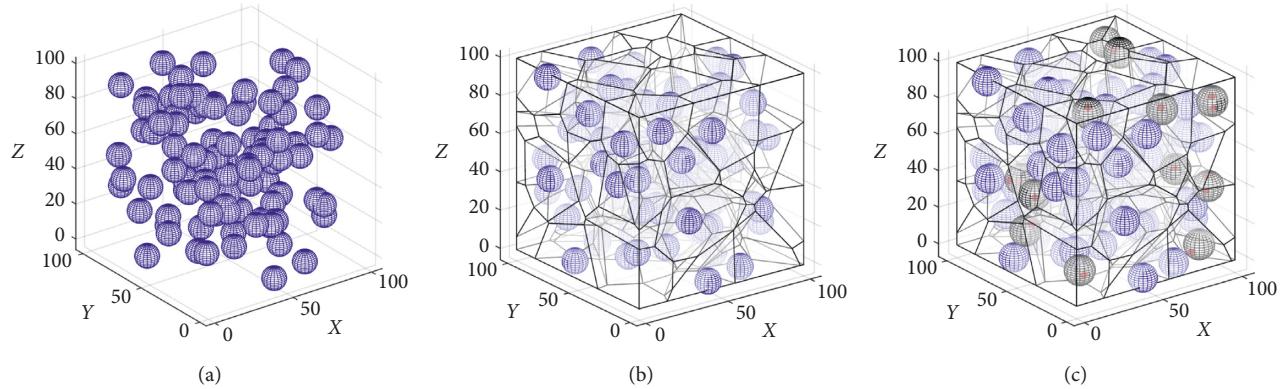

Figure 7: Second group simulation experiment diagram. (a) Node initial deployment diagram. (b) Experimental simulation process diagram. (c) Experimental simulation result diagram.

the same number of target points. Furthermore, it is concluded from the above tables that the RA algorithm does not reach full coverage under any conditions, but the overall network coverage ratio of the 3D-VPCA algorithm is significantly improved. Therefore, the proposed algorithm can also achieve better detection for multiple target points under the same number of nodes.

In the fifth set of experiments, we again verified the relationship between the node sensing range and network coverage ratio. In this experiment, the network coverage ratio of the three algorithms was compared by changing the node's sensing range under different node numbers and target points, as shown in Figures 10–12.

In the three experimental comparisons in this section, we verified the relationship between changing the sensing radius of the sensor nodes and determining the network coverage ratio of the deployment target point, as shown in Figures 10–12. As can be seen from the above figures, the sensing range of the node is mainly between 10 and 70. In the first section of the experiment, we set the number of nodes and the number of targets to 15 and 40 for, respectively, verification. The experimental results are shown in

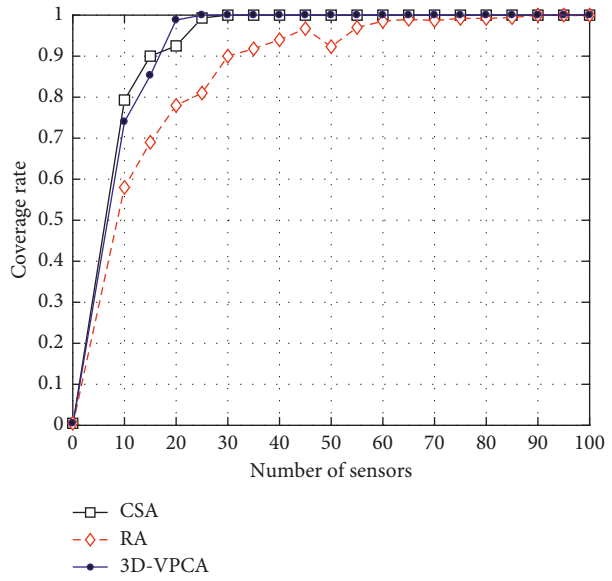

Figure 8: Algorithm comparison charts: target points set to 40.

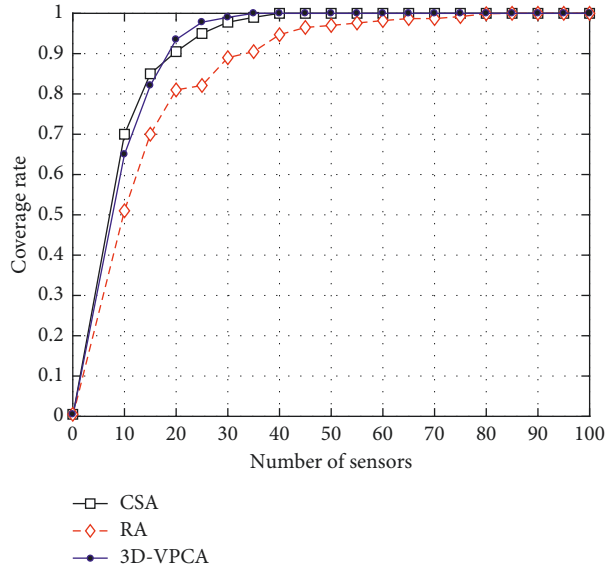

Figure 9: Algorithm comparison charts: target points set to 100.

Table 2: Comparison of indicators of three algorithms when the number of nodes is small.

Number of targets	RA			CSA			3D-VPCA		
	Min	Avg (%)	Max	Min	Avg (%)	Max	Min	Avg (%)	Max
10	4	87.33	10	10	100	10	10	100	10
20	15	87.33	20	20	100	20	20	100	20
30	23	86.66	30	30	100	30	30	100	30
40	28	88.25	39	39	99.91	40	40	100	40
50	39	88.13	48	49	99.33	50	50	100	50
60	47	88.39	59	57	98.61	60	58	99.72	60
70	52	86.90	69	66	97.28	70	67	97.53	70
80	64	88.17	75	76	97.50	80	76	97.50	80
90	73	88.15	87	85	96.96	90	85	96.96	90
100	75	89.10	98	95	97.40	100	96	97.49	100

Table 3: Comparison of indicators of three algorithms when the number of nodes is large.

Number of targets	RA			CSA			3D-VPCA		
	Min	Avg (%)	Max	Min	Avg (%)	Max	Min	Avg (%)	Max
10	7	89.33	10	10	100	10	10	100	10
20	16	91.83	20	20	100	20	20	100	20
30	23	91.22	30	30	100	30	30	100	30
40	34	93.75	40	40	100	40	40	100	40
50	39	91.87	49	50	100	50	50	100	50
60	45	88.94	59	59	99.94	60	60	100	60
70	61	93.28	69	66	99.90	70	70	100	70
80	68	90.87	80	76	99.37	80	78	99.48	80
90	75	92.41	88	87	99.25	90	89	99.41	90
100	81	91.90	99	98	99.43	100	99	99.53	100

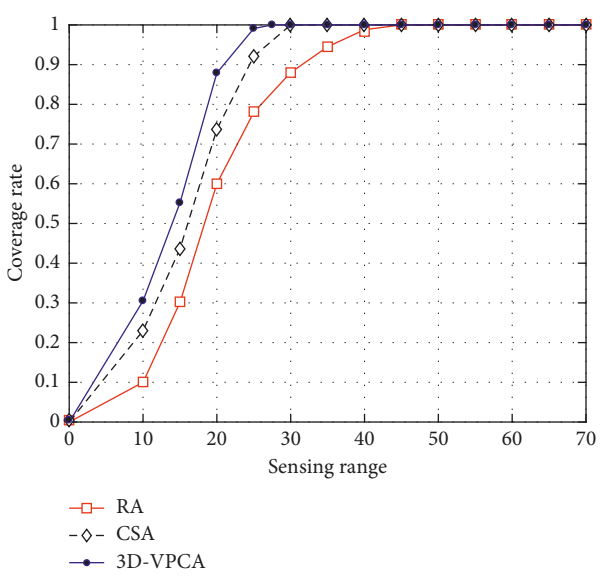

Figure 10: Sparsely deployed targets and nodes.

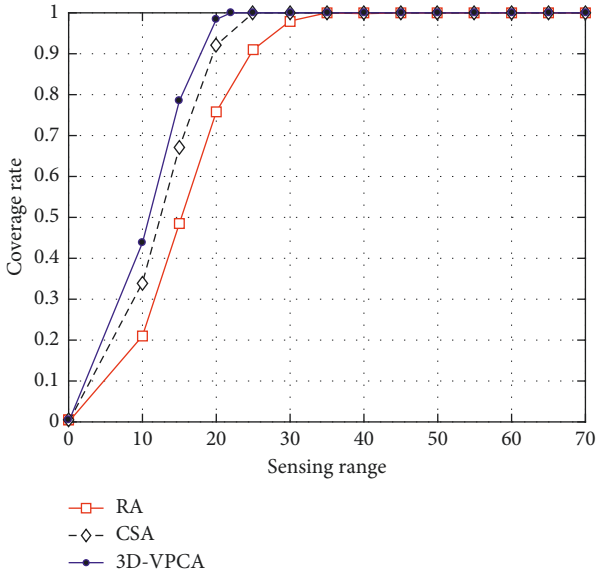

Figure 11: Densely deployed sensor nodes.

Figure 10. In the second experiment, we set the number of nodes and the number of targets to 60 and 100, respectively, for comparative analysis. The experimental results are shown in Figure 11. In the last experiment, we set the number of sensor nodes and target points to 10 and 100, respectively. The experimental results are shown in Figure 12. It can be concluded from the three experiments that as the node sensing radius increases, the coverage ratio of the three algorithms increases significantly. The blue line (e.g., Figure 10) represents the coverage ratio change of the 3D-VPCA algorithm. It can be seen that the coverage ratio is greater than that of the RA and CSA algorithms. Furthermore, it is concluded from Figure 10 that when the sensing range of the node is 27, the 3D-VPCA algorithm achieves full coverage faster than the other two algorithms. In the second part of Experiment 7 (e.g., Figure 11), when the number of nodes and the number of target points are increased, the coverage ratio of the three algorithms is increased compared with the coverage ratio of the three algorithms in the first part of experiment. On the contrary, the 3D-VPCA algorithm has the fastest growth ratio and is the first to achieve

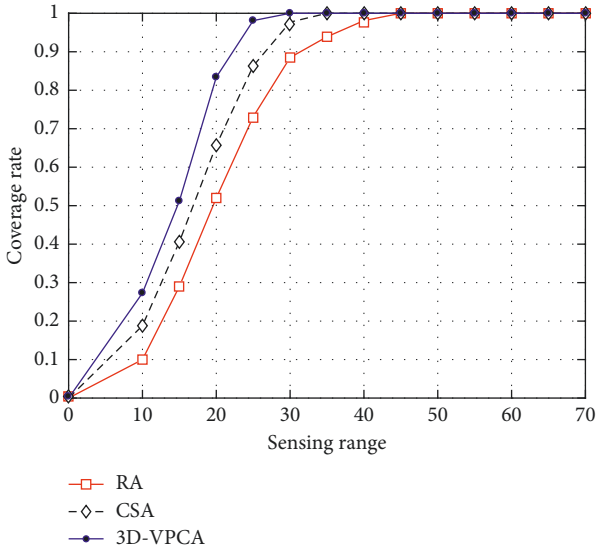

Figure 12: Densely deployed target points.

full coverage under the same conditions. As shown in Figure 11, when the sensing range is 22, the coverage ratio of the 3D-VPCA algorithm reaches 1 first and the coverage growth is superior to that of the other two algorithms. In the last part of the experiment (e.g., Figure 12), when the number of nodes is small and the number of target points is large, the coverage ratio growth of the three algorithms is significantly smaller than that of the previous two experiments.

Therefore, through experimental comparison of the three algorithms, the following conclusions can be drawn:

(i) When the number of sensor nodes and target points is determined, the coverage ratio of the three algorithms under the same conditions increases and decreases with the sensing radius of the node.

(ii) Under the same conditions, when the node sensing radius is 25–30, the coverage ratio of the 3D-VPCA algorithm can reach more than 90%. When the node sensing radius is 30, the 3D-VPCA algorithm can achieve complete coverage.

(iii) The coverage ratio of the 3D-VPCA algorithm proposed in this paper is better than that of the CSA and RA algorithms under the same conditions.

7. Conclusion and Future Research

In this paper, we studied the coverage of target events in WSNs. For the requirements of random coverage of nodes in a 3D environment and node deployment under some special circumstances in a real environment, we proposed a 3D-VPCA algorithm and applied it to target coverage optimization in 3D WSNs. First, we constructed a network model and introduced a three-dimensional Voronoi partitioning method to construct '*V*-body' units to improve the network coverage ratio and node utilization. Second, related algorithms were proposed for theoretical analysis and verification. Finally, the 3D-VPCA algorithm and two other algorithms were analysed and compared through numerous experiments. The results showed that the 3D-VPCA algorithm can significantly reduce the network energy consumption and achieve a higher coverage ratio. In the future, we will further study some key issues in WSNs, such as the mobility of target events and related algorithms. In addition, we will conduct relevant tests in an actual environment.

Data Availability

The data used to support the findings of this study are available from the corresponding author upon request.

Conflicts of Interest

The authors declare that there are no conflicts of interest regarding the publication of this paper.

Acknowledgments

This work was supported by the National Natural Science Foundation of China (61762079 and 61662070) and Key Science and Technology Development Program of Gansu Province (1604FKCA097 and 17YF1GA015).

References

[1] N. Boufares, I. Khoufi, P. Minet, L. Saidane, and Y. B. Saied, "Three- dimensional mobile wireless sensor networks redeployment based on virtual forces," in *Proceedings of the 2015 International Wireless Communications and Mobile Computing Conference (IWCMC)*, pp. 563–568, Dubrovnik, Croatia, August 2015.

[2] M. R. Senouci, A. Mellouk, K. Asnoune, and F. Y. Bouhidel, "Movement-Assisted sensor deployment algorithms: a survey and taxonomy," *IEEE Communications Surveys & Tutorials*, vol. 17, no. 4, pp. 2493–2510, 2015.

[3] T. Wang, Z. Peng, C. Wang et al., "Extracting target detection knowledge based on spatiotemporal information in wireless sensor networks," *International Journal of Distributed Sensor Networks*, vol. 12, no. 2, Article ID 5831471, 2016.

[4] M. R. L. F. E. Silva, G. H. S. D. Carvalho, D. C. Monteiro, and L. S. Machado, "Distributed target location in wireless sensors network: an approach using FPGA and artificial neural network," *Wireless Sensor Network*, vol. 7, no. 5, pp. 35–42, 2015.

[5] P. Kumar and H.-J. Lee, "Security issues in healthcare applications using wireless medical sensor networks: a survey," *Sensors*, vol. 12, no. 1, pp. 55–91, 2011.

[6] O. D. Incel, A. Ghosh, B. Krishnamachari, and K. Chintalapudi, "Fast data collection in tree-based wireless sensor networks," *IEEE Transactions on Mobile Computing*, vol. 11, no. 1, pp. 86–99, 2012.

[7] X. Xing, G. Wang, and J. Li, "Polytype target coverage scheme for heterogeneous wireless sensor networks using linear programming," *Wireless Communications and Mobile Computing*, vol. 14, no. 14, pp. 1397–1408, 2014.

[8] W. Wang, V. Srinivasan, K. C. Chua, and B. Wang, "Energy-efficient coverage for target detection in wireless sensor networks," in *Proceedings of the 6th International Conference on Information Processing in Sensor Networks*, pp. 313–322, ACM, Cambridge, MA, USA, April 2007.

[9] R. Tan, G. Xing, J. Wang, and H. C. So, "Exploiting reactive mobility for collaborative target detection in wireless sensor networks," *IEEE Transaction on Mobile Computing*, vol. 9, no. 3, pp. 317–332, 2010.

[10] M. Abdelkader, M. Hamdi, and N. Boudriga, "Multi-target tracking using wireless sensor networks based on higher-order voronoi diagrams," *Journal of Networks*, vol. 4, no. 7, pp. 589–597, 2009.

[11] Z. Liao, S. Zheng, J. Cao, W. Wang, and J. Wang, "Minimizing movement for target coverage in mobile sensor networks," in *Proceedings of the 2012 32nd International Conference on Distributed Computing Systems Workshops (ICDCSW)*, pp. 194–200, IEEE, Macau, China, June 2012.

[12] H. J. Lee, Y. H. Kim, Y. H. Han, and C. Y. Park, "Centroid-based movement assisted sensor deployment schemes in wireless sensor networks," in *Proceedings of the IEEE 70th, Vehicular Technology Conference Fall*, pp. 1–5, Anchorage, AK, USA, September 2009.

[13] A. Iliodromitis, G. Pantazis, and V. Vescoukis, "2D wireless sensor network deployment based on Centroidal Voronoi Tessellation," *AIP Conference Proceedings*, vol. 1836, no. 1, 2017.

[14] Q. Zhang and M. Fok, "A two-phase coverage-enhancing algorithm for hybrid wireless sensor networks," *Sensors*, vol. 17, no. 12, p. 117, 2017.

[15] P. Medagliani, J. Leguay, G. Ferrari, V. Gay, and M. Lopez-Ramos, "Energy-efficient mobile target detection in wireless sensor networks with random node deployment and partial coverage," *Pervasive and Mobile Computing*, vol. 8, no. 3, pp. 429–447, 2012.

[16] Y. Hu, M. Dong, K. Ota, A. Liu, and M. Guo, "Mobile target detection in wireless sensor networks with adjustable sensing frequency," *IEEE Systems Journal*, vol. 10, no. 3, pp. 1160–1171, 2016.

[17] X. Yang, "A collision-free self-deployment of mobile robotic sensors for three-dimensional distributed blanket coverage control," in *Proceedings of the 2017 IEEE International Conference on Robotics and Bio mimetics (ROBIO)*, pp. 80–85, Macau, China, December 2017.

[18] J. Zhang, R. Wang, Y. Qian, and Q. Wang, "A coverage control algorithm based on probability model for three-dimensional wireless sensor networks," in *Proceedings of the 11th International Symposium on Distributed Computing and Applications to Business, Engineering & Science (DCABES)*, pp. 169–173, Guilin, China, 2012.

[19] L. Tan, C. Yang, X. Tang, and Y. Jiao, "A target tracking algorithm based on path virtual force," in *Proceedings of the IEEE International Conference on Computational Science and Engineering*, vol. 1, pp. 512–517, Guangzhou, China, 2017.

[20] V. Nazarzehi and A. V. Savkin, "Decentralized control of mobile three-dimensional sensor networks for complete coverage self-deployment and forming specific shapes," in *Proceedings of the IEEE Conference on Control Application*, (CCA), Sydney, NSW, Australia, pp. 127–132, 2015.

[21] L. Feng, Z. Sun, and T. Qiu, "Genetic algorithm-based 3d coverage research in wireless sensor networks," in *Proceedings of the 2013 Seventh International Conference on Complex, Intelligent, and Software Intensive Systems (CISIS)*, Taichung, Taiwan, pp. 633–628, 2013.

[22] G. Wang, G. Cao, and T. F. La Porta, "Movement-assisted sensor deployment," *IEEE Transactions on Mobile Computing*, vol. 5, no. 6, pp. 640–652, 2006.

[23] G. Li and S. Hu, "Coverage optimization algorithm based on VF-CS in mobile sensor network," *Journal on Communications*, vol. 39, pp. 95–107, 2018, in Chinese.

[24] L. M. Wang, F. Li, and Y. Qin, "Resilient method for recovering coverage holes of wireless sensor networks by using mobile nodes," *Journal on Communications*, vol. 32, pp. 1–8, 2011, in Chinese.

[25] P. Sahoo, H. Thakkar, and I.-S. Hwang, "Pre-scheduled and self organized sleep-scheduling algorithms for efficient K-coverage in wireless sensor networks," *Sensors*, vol. 17, no. 12, p. 2945, 2017.

[26] H. Zhang and J. C. Hou, "Maintaining sensing coverage and connectivity in large sensor networks," *Ad Hoc and Sensor Wireless Networks*, vol. 1, pp. 89–124, 2005.

[27] P. Kumar Sahoo, M.-J. Chiang, and S.-L. Wu, "An efficient distributed coverage hole detection protocol for wireless sensor networks," *Sensors*, vol. 16, no. 3, p. 386, 2016.

[28] A. Boukerche and X. Fei, "A voronoi approach for coverage protocols in wireless sensor networks," in *Proceedings of the Global Telecommunications Conference*, pp. 5190–5194, IEEE, Washington, DC, USA, November 2007.

[29] A. Howard, M. J. Matarić, and G. S. Sukhatme, "Mobile sensor network deployment using potential fields: a distributed, scalable solution to the area coverage problem," in *Proceedings of the Distributed Autonomous Robotic Systems*, pp. 299–308, Springer, Fukuoka, Japan, June 2002.

[30] H. Liu, Z. J. Chai, J. Z. Du, and B. Wu, "Sensor redeployment algorithm based on combined virtual forces in three-dimensional space," *Acta Automatica Sinica*, vol. 37, pp. 713–723, 2011.

[31] P. Jiang, Y. Xu, and J. Liu, "A distributed and energy-efficient algorithm for event k-coverage in underwater sensor networks," *Sensors*, vol. 17, no. 12, p. 186, 2017.

[32] Z. Zhou, S. R. Das, and H. Gupta, "Variable radii connected sensor cover sensor in sensor networks," *ACM Transaction on Sensor Networks*, vol. 5, p. 8, 2009.

[33] S. Ahmed, N. Javaid, F. A. Khan et al., "Co-UWSN: co-operative energy-efficient protocol for underwater WSNs," *International Journal of Distributed Sensor Networks*, vol. 11, no. 4, Article ID 891410, 2015.

[34] D. Arivudainambi, S. Balaji, and T. S. Poorani, "Sensor deployment for target coverage in underwater wireless sensor network," in *Proceedings of the 2017 International Conference on Performance Evaluation and Modeling in Wired and Wireless Networks (PEMWN)*, pp. 1–6, IEEE, Paris, France, July 2017.